

Comparison of Ray-tracing and Full-wave Code Modeling of Helicon Heating and Current Drive in DIII-D*

R.I. Pinsker¹, N. Bertelli², D.L. Green³, E.F. Jaeger⁴, C.H. Lau³, J.M. Park³,
M. Porkolab⁵ and R. Prater¹

¹*General Atomics, P.O. Box 85608, San Diego, CA 92186-5608, USA*

²*Princeton Plasma Physics Laboratory, P.O. Box 451, Princeton, NJ 08543-0451, USA*

³*Oak Ridge National Laboratory, P.O. Box 2008, Oak Ridge, TN 37831, USA*

⁴*XCEL Engineering, Inc., Oak Ridge, TN 37830, USA*

⁵*MIT Plasma Science and Fusion Center, Cambridge, MA 02139, USA*

An experimental test of mid-radius current drive using the “helicon” (also known as the “whistler”) wave at 476 MHz is being carried out on the DIII-D tokamak to determine the efficiency of coupling to this wave and to test the predicted high current drive efficiency [1]. Up to now, an important open question for this wave has been whether the radial location of the damping and current drive can be controlled by varying the launched parallel index of refraction n_{\parallel} . While ray-tracing calculations [1] predict that the radial location of the helicon damping and current drive is almost independent of the launched parallel wavenumber, very much more computationally expensive full-wave code analyses with STELION [2] have suggested a possible dependence of the radial location of the deposition on the launched parallel wavenumber. In this paper, full-wave solutions of helicon waves launched with a single toroidal mode number obtained with the AORSA code [3] are compared with ray-tracing results from GENRAY [4] in order to investigate this issue.

The reason that the ray-tracing studies show almost no dependence of minor radius of the deposition location on the launched n_{\parallel} (within the limits imposed by wave accessibility at low $|n_{\parallel}|$ and practicality of launch at high $|n_{\parallel}|$) was explained in [5]. The whistler wave ray trajectories make only a small angle with the static magnetic field lines, so to lowest order the rays follow the field lines around the torus, with slow radial penetration. However, unlike the slow wave (“lower hybrid”) branch, where that small angle between the rays and the field lines is almost independent of n_{\parallel} , leading to resonance-cone behavior, the fast branch (“helicon” or “whistler”) rays make a steeper angle with the field lines as $|n_{\parallel}|$ is increased. The higher the value of $|n_{\parallel}|$, the lower the energy of electrons that are Landau resonant with the waves, so if everything were equal, the higher $|n_{\parallel}|$ waves would damp at lower electron temperatures and hence at larger minor radius. (This is what happens with the lower hybrid branch.) But for the whistler, the more rapid radial penetration of the rays that results from the higher $|n_{\parallel}|$ largely compensates for the higher damping per unit length along the trajectory, with the result being that for a range of $|n_{\parallel}|$ the damping occurs at roughly the same minor radius. In the high-performance DIII-D discharge studied in [1], GENRAY predicts that the damping and current drive would occur at normalized minor radius $0.55 < \rho < 0.6$ as the launched n_{\parallel} is varied over $2.8 < n_{\parallel} < 4.2$. The comparison between a ray starting with $n_{\parallel}=3$ and

$n_{\parallel}=4$ is shown in Figs. 1 and 2; the steeper angle at which the ray crosses the flux surfaces at higher initial n_{\parallel} is visible in the poloidal projection, while the absorption is stronger earlier in the ray trajectory, leading to a broader deposition profile than is obtained with the lower initial n_{\parallel} . However, the slower radial penetration the latter case yields a more rapid absorption and a more radially peaked deposition once n_{\parallel} and the local electron temperature have risen to a value at which Landau damping sets in. The n_{\parallel} hardly rises early in the trajectory, especially for the slowly penetrating $n_{\parallel}=3$ case, because the major radius of the ray decreases only slowly with the above-midplane launch position and the nearly vertical flux surfaces in the outside midplane region. The magnitude of n_{\parallel} begins to rise only after the field line and hence the ray gets below the midplane and the flux surfaces begin to curve towards smaller major radius. (To lowest order, $|n_{\parallel}|R \sim \text{constant}$.)

We expect ray-tracing to be valid in much of the plasma volume, because the helicon's perpendicular wavelength is quite short compared to the scale lengths over which the plasma parameters vary, once the wave is propagating. For example, at 0.5 GHz, density of $4 \times 10^{19} \text{ m}^{-3}$, $B_T=1.4 \text{ T}$, deuterium plasma at $n_{\parallel}=3$, the helicon has a perpendicular wavelength of about 1 cm ($k_{\perp} \sim 630 \text{ m}^{-1}$, or $n_{\perp}=k_{\perp}/k_0 \sim 60$ with $k_0=\omega/c$), while at $n_{\parallel}=4$, the perpendicular wavelength is 1.4 cm ($k_{\perp} \sim 450 \text{ m}^{-1}$, $n_{\perp} \sim 43$). This is much shorter than the density gradient scale length in DIII-D except at the very edge of the plasma, where the wave has just become propagating and the ray-tracing approximation is invalid in any event. Since the ray must be started within the domain in which the local approximation is valid, the problem of excitation of the waves with a realistic launcher located outside the plasma, where the waves are evanescent, must be addressed with a full-wave calculation like AORSA. In the work presented here, however, we are interested in the wave propagation and absorption in the core, and so do not use a realistic antenna or scrape-off layer model. Calculations of antenna

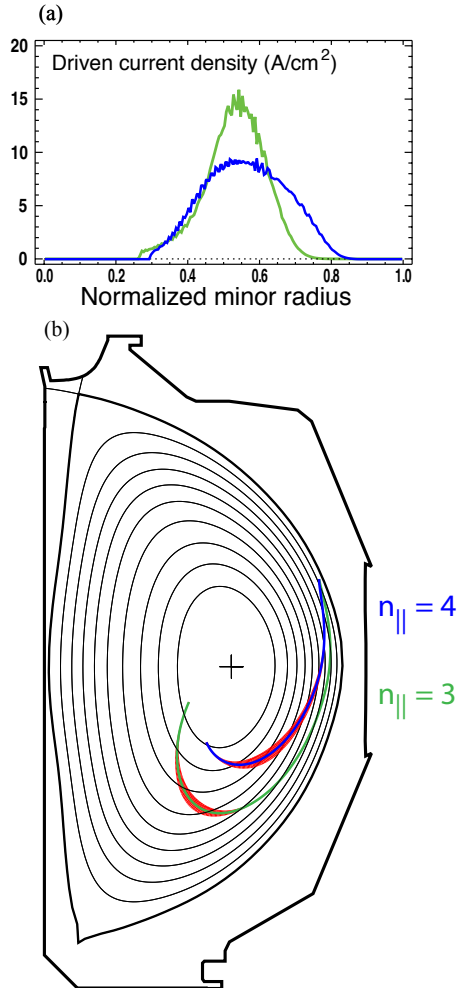


Figure 1. (a) Driven current profile as a function of normalized minor radius for ray with initial n_{\parallel} of 3 (green) and 4 (blue), in DIII-D equilibrium 122976 calculated by GENRAY. (b) Poloidal projection of ray paths for the two cases, with the thickness of the red shaded regions proportional the rate of absorption along the ray path, $(-1/P)(dP/ds)$.

loading in which the antenna is placed in a model of the scrape-off layer are being performed with AORSA and are described elsewhere [6].

In spectral codes such as AORSA, practical limits on computer memory and on computation time determine how fine the computational grid in wavenumber space can be, in turn setting the limit the minimum wavelength perpendicular to the primarily toroidal static magnetic field lines that can be modeled. Since for fast waves the perpendicular wavenumber scales as $k_{\perp} \sim \omega/v_A \sim f n_e^{0.5} B_0^{-1}$, high frequency, high density and low toroidal field all tend to make the required k_{\perp} high and a dense grid is needed. For this DIII-D case, the maximum density of the deuterium plasma is nearly $1 \times 10^{20} \text{ m}^{-3}$, so the maximum value of k_{\perp} is in the range $1000-1500 \text{ m}^{-1}$ (n_{\perp} in the range 95-143). The largest perpendicular wavenumber that can be resolved is $2\pi n_{\max}/\Delta L$, where ΔL is the dimension of the computational volume in the relevant direction and the grid in that direction has n_{\max} points. The finest grid that has been used so far on this problem is (400,400) (major radius, height), and those dimensions for DIII-D are roughly $(\Delta R, \Delta Z) \sim (1.4 \text{ m}, 2.5 \text{ m})$, hence maximum $(k_R, k_Z) \sim (1800 \text{ m}^{-1}, 1000 \text{ m}^{-1})$. We compute the values of the perpendicular index of refraction n_{\perp} along the GENRAY ray path with the results shown as the heavy line in the top panels of Fig. 3, where it is evident that the maximum n_{\perp} encountered along the ray path is about 85 for the case with an initial $n_{\parallel}=3$, and a less marginal value of about 60 for the case with initial $n_{\parallel}=4$. We therefore anticipate a better agreement between AORSA results with a 400 by 400 grid and GENRAY results for the latter case. Contours of the wave electric field amplitude from the two AORSA runs are compared with the GENRAY ray path in the lower panels of Fig. 3, and indeed the maximum wave amplitudes from AORSA coincide with the ray path for the case of higher initial n_{\parallel} , while in the other case, the AORSA fields appear to penetrate the flux surfaces slightly more rapidly than the ray path. This was further investigated by carrying out a local Fourier transform of the AORSA wave fields along the GENRAY path and comparing the perpendicular wavenumber spectrum with the GENRAY values. This analysis, shown in the top panels of Fig. 3, verifies that the lower values of n_{\perp} needed for the higher n_{\parallel} case are faithfully reproduced by AORSA, while the AORSA spectrum saturates at a level slightly lower than the maximum n_{\perp} required for the other case.

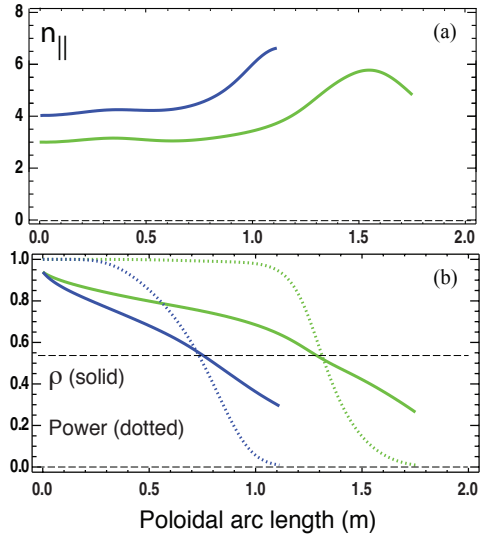


Figure 2. (a) n_{\parallel} evolution along the two rays shown in Fig. 1. (b) Normalized minor radius ρ along the rays (solid lines) and the normalized power remaining in the rays (dotted). Color code same as in Fig. 1. The horizontal dashed line drawn at $\rho=0.55$ shows that the peak in the absorption occurs at almost the same minor radius in the two cases.

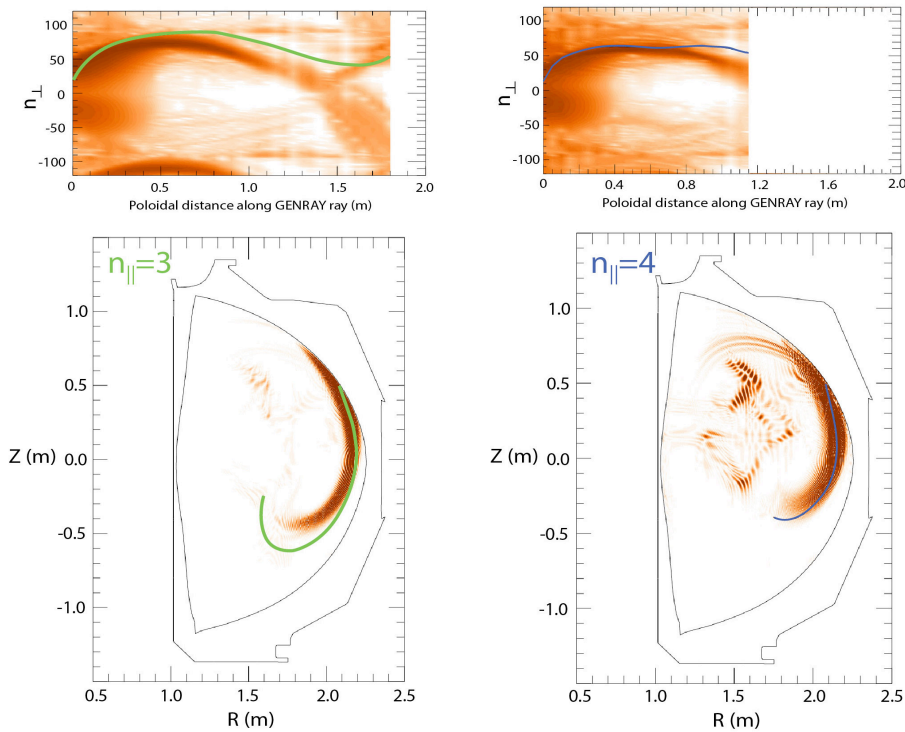


Figure 3. Comparison of ray paths from GENRAY with field ($|E_{rf}|$) contours from AORSA for initial values of $n_{\parallel}=3$ (lower left) and $n_{\parallel}=4$ (lower right). The upper panels show the Fourier spectrum of the AORSA fields for n_{\perp} at each point along the GENRAY-computed ray path, parameterized by the poloidal distance along the path, compared with GENRAY's computed n_{\perp} along the ray. Darker colors of the contours correspond to larger field or Fourier amplitudes.

Therefore good agreement between the predicted driven current profiles from the two different computational approaches for the $n_{\parallel}=4$ case reported in [5] is consistent with these results, while to get similarly good agreement with the lower value of n_{\parallel} may require a finer grid and significantly more computer time. We conclude that in this regime, ray-tracing provides a computationally cheap and accurate tool for analysis of current drive with helicon waves, but that it should be spot-checked with the more complete full-wave model to the extent that available computational resources permit.

This work was supported in part by the US Department of Energy under DE-FC02-04ER54698, DE-AC02-09CH11466, and DE-AC05-00OR22725.

- [1] R. Prater, C.P. Moeller, R.I. Pinsker, *et al.*, Nucl. Fusion **54**, 083024 (2014)
- [2] V. Vdovin, Plasma Phys. Reports **39**, 95 (2013).
- [3] E.F. Jaeger, L.A. Berry, E. D'Azevedo, *et al.*, Phys. Plasmas **8**, 1573 (2001)
- [4] R.W. Harvey and A.P. Smirnov, *The GENRAY Ray Tracing Code*, CompX Rep. CompX-2000-01 (2001).
- [5] R.I. Pinsker, R. Prater, C.P. Moeller, *et al.*, "Off-axis Current Drive With Very High Harmonic Fast Waves for DIII-D", Paper TH/P2-38, IAEA Fusion Energy Conference, St. Petersburg, RF, 2014, to be published in the proceedings.
- [6] C. Lau, E.F. Jaeger, N. Bertelli, *et al.*, in Proceedings of 21st Top. Conf. on RF Power in Plasmas, Lake Arrowhead, CA, April 27-29, 2015, to be published.